

A new search for the variation of fundamental constants using the rovibrational levels and isotope effects of the magnesium fluoride molecule

Di Wu(吴迪), Jin Wei(魏晋), Taojing Dong(董涛晶), Chenyu Zu(祖晨宇), Yong Xia(夏勇), and Jianping Yin(印建平)

Citation: Chin. Phys. B, 2025, 34 (**2**): 023101. DOI: 10.1088/1674-1056/ad990e
Journal homepage: http://cpb.iphy.ac.cn; http://iopscience.iop.org/cpb

What follows is a list of articles you may be interested in

Effect of conical intersection of benzene on non-adiabatic dynamics

Duo-Duo Li(李多多) and Song Zhang(张嵩)
Chin. Phys. B, 2022, 31 (**8**): 083103. DOI: 10.1088/1674-1056/ac5607

Dynamic polarizabilities of the clock states of Al^+

Yuan-Fei Wei(魏远飞), Zhi-Ming Tang(唐志明), Cheng-Bin Li(李承斌), Yang Yang(杨洋), Ya-Ming Zou(邹亚明), Kai-Feng Cui(崔凯枫), and Xue-Ren Huang(黄学人)
Chin. Phys. B, 2022, 31 (**8**): 083102. DOI: 10.1088/1674-1056/ac5880

Theoretical analysis of the coupling between Feshbach states and hyperfine excited states in the creation of $^{23}Na^{40}K$ molecule

Ya-Xiong Liu(刘亚雄), Bo Zhao(赵博)
Chin. Phys. B, 2020, 29 (**2**): 023103. DOI: 10.1088/1674-1056/ab6314

Stark-potential evaporative cooling of polar molecules in a novel optical-access opened electrostatic trap

Sun Hui (孙慧), Wang Zhen-Xia (王振霞), Wang Qin (王琴), Li Xing-Jia (李兴佳), Liu Jian-Ping (刘建平), Yin Jian-Ping (印建平)
Chin. Phys. B, 2015, 24 (**11**): 113101. DOI: 10.1088/1674-1056/24/11/113101

High-precision spectroscopy of hydrogen molecular ions

Zhong Zhen-Xiang (钟振祥), Tong Xin (童昕), Yan Zong-Chao (严宗朝), Shi Ting-Yun (史庭云)
Chin. Phys. B, 2015, 24 (**5**): 053102. DOI: 10.1088/1674-1056/24/5/053102

A new search for the variation of fundamental constants using the rovibrational levels and isotope effects of the magnesium fluoride molecule

Di Wu(吴迪)[1], Jin Wei(魏晋)[1], Taojing Dong(董涛晶)[1], Chenyu Zu(祖晨宇)[1], Yong Xia(夏勇)[1,2,3,†], and Jianping Yin(印建平)[1,‡]

[1] *State Key Laboratory of Precision Spectroscopy, School of Physics and Electronic Science, East China Normal University, Shanghai* 200241, *China*
[2] *Collaborative Innovation Center of Extreme Optics, Shanxi University, Taiyuan* 030006, *China*
[3] *NYU-ECNU Institute of Physics at NYU Shanghai, Shanghai* 200062, *China*

(Received 22 July 2024; revised manuscript received 19 November 2024; accepted manuscript online 2 December 2024)

The recently demonstrated methods for cooling and trapping diatomic molecules offer new possibilities for precision searches in fundamental physical theories. Here, we propose to study the variations of the fine-structure constant ($\alpha = e^2/(\hbar c)$) and the proton-to-electron mass ratio ($\mu = m_p/m_e$) with time by taking advantage of the nearly degenerate rovibrational levels in the electronic states of the magnesium fluoride (MgF) molecule. Specifically, due to the cancellation between the fine-structure splitting and the rovibrational intervals in the different MgF natural isotopes, a degeneracy occurs for $A^2\Pi_{3/2}$ $(v' = 0, J' = 18.5, -)$ and $A^2\Pi_{1/2}$ $(v'' = 0, J'' = 20.5, -)$. We find that using the nearly degenerate energy level of such states can be 10^4 times more sensitive than using a pure rotational transition to measure the variations of α and μ. To quantify the small gap between $A^2\Pi_{3/2}$ $(v' = 0, J' = 18.5, -)$ and $A^2\Pi_{1/2}$ $(v'' = 0, J'' = 20.5, -)$, special transitions of choice are feasible: $X^2\Sigma^+_{1/2}$ $(v = 0, J = 19.5, +)$ to $A^2\Pi_{3/2}$ $(v' = 0, J' = 18.5, -)$ and $X^2\Sigma^+_{1/2}$ $(v = 0, J = 19.5, +)$ to $A^2\Pi_{1/2}$ $(v'' = 0, J'' = 20.5, -)$. In addition, we estimate the frequency uncertainties caused by the narrow linewidth, Zeeman shift, Stark shift, Doppler broadening and blackbody radiation.

Keywords: cold molecule, proton-to-electron mass ratio, precision measurement

PACS: 31.30.Gs, 33.15.Pw, 37.10.Mn, 06.20.Jr

DOI: 10.1088/1674-1056/ad990e **CSTR:** 32038.14.CPB.ad990e

1. Introduction

In the Standard Model of particle physics, the fundamental constants are considered to be fixed parameters, but the theory that gravity unifies with other interactions suggests that the variations in time and space are the functions of the fundamental constants, which means that Einstein's equivalence principle is invalid.[1,2] The observed expansion of the Universe causes the constants to change with position and/or time. The theories of the scalar field of dark energy also predict the variation of the fundamental constants.[3–5] As mentioned in Ref. [6], many theories require the precise determination of the variation of the fundamental constants in time and space.[7,8] Thus, high-precision measurements of the variation of fundamental constants,[9–21] such as the fine-structure constant $\alpha = e^2/(\hbar c)$ and the proton-to-electron mass ratio $\mu = m_p/m_e$, will play an important role in answering these open questions in physics. Atoms and molecules are compact and naturally occurring systems that can be isolated from the external environment. We can choose the specific quantum states in an atom or a molecule, which are sensitive to measurement in the laboratory. Indeed, molecular species have rich internal degrees of freedom, large electric dipole moments and unique chemical characteristics, so they offer a powerful platform for the study of encoding and processing quantum information,[22–24] ultracold chemistry[25] and precision measurement.[26–28] For example, in Ref. [11], it was reported that a limit on the fractional temporal variation of the proton-to-electron mass ratio was $(-3.8 \pm 5.6) \times 10^{-14}$ yr^{-1} using a rovibrational transition in SF_6. In Ref. [12], using ultracold KRb molecules produced from laser-cooled atoms, the measurement reported the variation of electron-to-proton mass ratio $(1/\mu)$ to be $(0.3 \pm 1.0) \times 10^{-14}$ yr^{-1}. While various research groups have proposed methods employing atomic and molecular systems to measure the proton-to-electron mass ratio (m_p/m_e), the precise determination of fundamental physical constants remains an essential area of research. Independent measurements based on different theoretical and technological approaches are essential to verify the consistency of results, to reduce systematic errors and to increase the credibility of experimental results.

In this paper, we use the MgF molecule to search for the variation of α and μ. As shown in Ref. [29], the rovibrational resolved electronic transitions in a molecule system are sensitive to the variation of α and μ. There are already many

†Corresponding author. E-mail: yxia@phy.ecnu.edu.cn
‡Corresponding author. E-mail: jpyin@phy.ecnu.edu.cn

© 2025 Chinese Physical Society and IOP Publishing Ltd. All rights, including for text and data mining, AI training, and similar technologies, are reserved.

proposed theories and experiments using different diatomic molecules to validate each other.[30–36] Here, we present detailed studies to search for the variation of α and μ using the nearly degenerate energy levels in MgF. The production of MgF using laser ablation and buffer gas cooling has been reported in Refs. [37,38]. Compared to previous reports, there are several advantages to using MgF as a viable probe. First, precise spectral lines and spectrum constants have been observed and fitted in Refs. [37–39], and MgF is a good candidate for laser cooling and trapping.[40–43] Second, the selected optical transitions have a small uncertainty — two orders of magnitude lower than in the microwave domain under the same conditions.[44] Third, the interval between the nearly degenerate energy levels is about 100 MHz, which can contribute to considerably more sensitivity — a factor of 10^4 — in future experiments. Based on these advantages, MgF emerges as a strong candidate molecule for probing the variation of α and μ.

2. Sensitivity of molecular electronic state transitions to the variation of α and μ

The dependence of molecular constants on μ can be expressed by the scaling relations upon isotopic substitution.[45] The harmonic constant ω_e and the rotational constant B_e are proportional to μ and the ratios are $-1/2$ and -1, respectively. Diatomic molecules with nearly degenerate rovibrational energy levels are particularly sensitive to variation of the fundamental constants with time, and there will be great enhancement.[10,29] After taking into account the cancellation between fine-structure splits and rovibrational intervals, the enhancement is truly there. The fine-structure interval ω_f has a direct relation with the fine-structure constant $\alpha = e^2/(\hbar c)$, as $\omega_f \sim Z^2\alpha^2 E_H$, where Z is the nuclear charge and $E_H = m_e e^4/\hbar^2$ is the Hartree atomic energy unit. On the other hand, the vibration energy decreases with the atomic mass: $\omega_v \sim M_r^{-\frac{1}{2}}\mu^{-\frac{1}{2}}E_H$, where m_p is the proton mass and M_r is the reduced mass for the molecular vibration.[29] Therefore, the cancellation between the fine-structure split and the vibrational interval can be expressed as follows:

$$\omega = \omega_f - v\omega_v \approx 0, \quad v = 1, 2, \ldots. \tag{1}$$

In addition, the rotational constant B_e is also related to μ. If we consider the energy level interval between two states like $(\Omega = 3/2, v'' = 0, J'' = j)$ and $(\Omega = 1/2, v' = 0, J' = j+2)$ $(\Delta J = 2)$, with the increase in rotational quantum number, the rotational energy will make a difference. So, concerning the contribution from the rotational energy, it can expressed as follows:

$$\omega = \omega_f - v\omega_v - 4JB_v \approx 0, \quad v = 0, 1, \ldots, \quad J = 1, 2, \ldots, \tag{2}$$

where v and J are the vibrational quantum number and rotational quantum number, respectively, and B_v is the rotational constant for the vibrational level v and can be approximately expressed as $B_e - \alpha_e(v+1/2)$. B_e is the rotational constant for the vibrational level $v = 0$ and α_e is the parameter Y_{11} in the Dunham model.[46]

Considering the energy level interval between two states like $\left(A\Pi_{3/2}, v'' = 0, J'' = j\right)$ and $\left(A\Pi_{1/2}, v' = 0, J' = j+2\right)$, the cancellation between fine-structure multiples and rovibrational intervals can be expressed as

$$\omega = \omega_f - 4JB_v \approx 0. \tag{3}$$

The fractional variation of ω can be expressed as

$$\begin{aligned} \frac{\delta\omega}{\omega} &= \frac{1}{\omega}\left(2\omega_f\frac{\delta\alpha}{\alpha} + 4JB_v\frac{\delta\mu}{\mu}\right) \\ &\approx K\left(2\frac{\delta\alpha}{\alpha} + \frac{\delta\mu}{\mu}\right), \end{aligned} \tag{4}$$

where $K = \frac{\omega_f}{\omega_f - 4JB_v} = \frac{\omega_f}{\omega}$ is the enhancement factor representing the sensitivity. Since α_e is far smaller than B_e, we ignore the α_e term. The enhancement factor can thus be expressed as $K = \frac{\omega_f}{\omega_f - 4JB_e}$. Because of the cancellation between the fine-structure split and the rovibrational intervals, the energy level spacing ω is near zero, so it turns out that $|K|$ can be quite dramatic, even several orders of magnitude. In the following sections, we will use Eq. (4) to calculate the sensitivity, K, from the nearly degenerate electronic states.

3. Isotope effect and energy level configuration in MgF molecules

The energy level configuration of ground electronic state $X^2\Sigma^+_{1/2}$ in $^{24}Mg^{19}F$ has been studied in detail.[41] The spectrum constants of the ground electronic state $X^2\Sigma^+_{1/2}$ in $^{25}Mg^{19}F$ and $^{26}Mg^{19}F$ have been fitted.[39] In Ref. [47], the rotational constants and Λ-doubling constants of $A^2\Pi$ have been studied. For the spectrum constants of $A^2\Pi$ in $^{25}Mg^{19}F$ and $^{26}Mg^{19}F$, we could use the isotopic dependence theory to investigate.[48]

The treatment applies to the vibration–rotation effects in diatomic molecules in singlet electronic states based on the Dunham expansion, which can be expressed as follows:

$$E(v, J) = hc\sum_{kl} Y_{kl}\left(v + \frac{1}{2}\right)^k [J(J+1)]^l, \tag{5}$$

where v and J are the vibrational and rotational quantum numbers, respectively.[49] The Dunham coefficient Y_{kl} is approximately as follows:

$$Y_{kl} \cong \mu_m^{-(k+2l)/2} U_{kl}, \tag{6}$$

where U_{kl} is isotopically invariant and μ_m is the reduced mass of molecules with different isotopes. Using Eq. (6), we could

estimate the different MgF isotopic Dunham coefficients by means of the known isotopic Dunham coefficients. The rotational constant (B_v) and the centrifugal distortional constant (D_v) of $X^2\Sigma^+_{1/2}$ and $A^2\Pi$ in $^{25}Mg^{19}F$ and $^{26}Mg^{19}F$ have been calculated using Eq. (6) and are listed in Tables 1 and 2.

Table 1. Rotational constants and centrifugal distortional constants of $X^2\Sigma^+_{1/2}$ in different MgF isotopes.

Molecular constant	$^{24}Mg^{19}F$ fitted (MHz)	$^{25}Mg^{19}F$ fitted (MHz)	$^{26}Mg^{19}F$ fitted (MHz)	$^{25}Mg^{19}F$ calc (MHz)	$^{26}Mg^{19}F$ calc (MHz)
B_v	15496.812	15223.127	14971.406	15222.915	14970.0872
D_v	0.032328	0.031365	0.030170	0.031195	0.030168

Table 2. Rotational constants and centrifugal distortional constants of $A^2\Pi$ in different MgF isotopes.

Molecular constant	$^{24}Mg^{19}F$ fitted (MHz)	$^{25}Mg^{19}F$ fitted (MHz)	$^{26}Mg^{19}F$ fitted (MHz)
B_e	15571.5201	15296.3025	15042.2555
D_e	0.01139	0.01119	0.01100

The coupling rules in the $X^2\Sigma^+_{1/2}$ state vary between different Mg isotopes. For the even Mg isotopes, the energy levels for the rotational levels of the $X^2\Sigma^+_{1/2}$ state are near the Hund's case $(b_{\beta J})$.[38] For the odd isotope ^{25}Mg, there are two coupling schemes.[50–52] The usual scheme is that the hyperfine interaction is smaller than the spin–rotation coupling, so the logical choice of basis set is

$$S+N=J,\ \ I_1+J=F_1,\ \ F_1+I_2=F, \tag{7}$$

which corresponds to the basis set as

$$|\eta\Lambda\rangle\,|N(SI_1)G(NG)F_1(F_1I_2)F\rangle\,,$$

where I_1 is the nuclear spin of the ^{25}Mg atom, equal to 5/2, and I_2 is the nuclear spin of ^{19}F atom, equal to 1/2. In the second scheme, if the Fermi contact hyperfine interaction is large, the logical choice of basis set is

$$S+I_1=G,\ \ N+G=F_1,\ \ F_1+I_2=F, \tag{8}$$

which corresponds to the basis set as

$$|\eta\Lambda\rangle\,|(NS)J(JI_1)F_1(F_1I_2)F\rangle\,,$$

called case $(b_{\beta S})$.

Using the parameters of the $X^2\Sigma^+_{1/2}$ state in $^{25}Mg^{19}F$ ($v=0$),[39] the Fermi contact parameter is larger than the spin–rotation parameter. As mentioned in Ref. [50], the Fermi coupling splitting is independent of the rotational quantum number N. Nevertheless, the contribution of the spin–rotation coupling increases with the rotational quantum number N. Thus, for low rotational levels, the coupling rule is approximate to Hund's case $(b_{\beta S})$. With an increase in N, the spin–rotation coupling will be larger than the Fermi contact. Consequently, the coupling rule will transform from Hund's case $(b_{\beta S})$ to Hund's case $(b_{\beta J})$. The energy level pattern of the $X^2\Sigma^+_{1/2}$ ($v=0$) state in $^{25}Mg^{19}F$ as a function of rotation is illustrated in Fig. 1. As shown in Fig. 1, with $N=15$, the coupling rule has transformed from Hund's case $(b_{\beta S})$ to Hund's case $(b_{\beta J})$. Thus, we use Hund's case $(b_{\beta J})$ to calculate the effective Hamiltonian of the $X^2\Sigma^+_{1/2}$ ($v=0$) state in $^{25}Mg^{19}F$ with $N=20$.

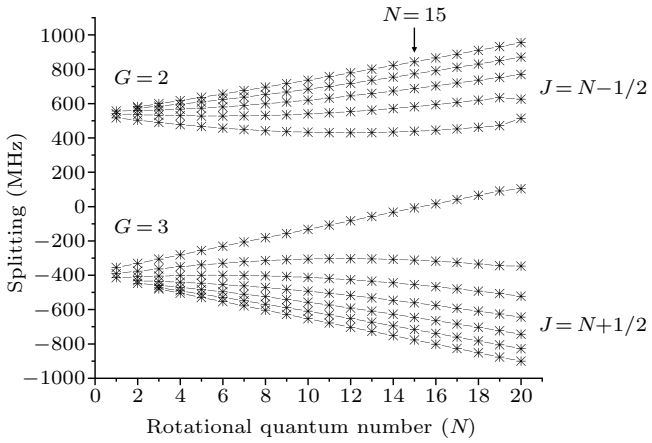


Fig. 1. Spin–rotation and hyperfine energy levels as a function of rotational quantum number N for the $X^2\Sigma^+_{1/2}$ ($v=0$) state in $^{25}Mg^{19}F$.

For a $A^2\Pi$ state, the total Hamiltonian can be expressed as

$$H^{\rm eff}\left(^2\Pi\right)=H_{\rm vib}+H_{\rm so}+H_{\rm LD}+H_{\rm rot}, \tag{9}$$

where $H_{\rm vib}$, $H_{\rm so}$, $H_{\rm LD}$ and $H_{\rm rot}$ are the vibronic Hamiltonian, spin–orbit coupling interaction, Λ-doubling Hamiltonian and rotational Hamiltonian, respectively. The analysis of the spectrum is accomplished using a case (a) basis although the increasing tendency towards case (b) coupling as J increases must be taken into account. It is customary to take the spin–orbital and rigid body rotation terms together.[46]

4. Constructing the narrow, close-lying levels of MgF

To construct the narrow, close-lying levels of MgF, we focus on constructing the close-lying levels of different MgF isotopes. According to Ref. [53], such levels may occur due to the cancellation between either hyperfine and rotational structures, or between the fine and vibrational structures. In MgF molecules, the spin–orbit coupling constant A_v is about 36 times larger than the adjacent rotational levels, so such levels may occur due to the cancellation between the fine-structure split and the rovibrational intervals of the two Π states (split by the Ω-ladders). The components of the total electronic angular momentum along the internuclear axis Ω take on the values $|\Lambda+\Sigma|=1/2,\ 3/2$, resulting in two Ω-ladders. Each J-level is split by the Λ-doubling into two components with opposite parity. The Λ-doubling in the $\Omega=1/2$ state is larger

than the Λ-doubling in the $\Omega = 3/2$ state. The rotational energy levels of the $A^2\Pi$ and $X^2\Sigma^+_{1/2}$ states are shown in Fig. 2, together with the selected transitions and close-lying levels. The notations here for the rotational transitions from $X^2\Sigma^+_{1/2}$ to $A^2\Pi$ are labeled as $T_{ab}(N)$. Thus, in Fig. 2, though the transition between $A^2\Pi_{1/2}$ $(v' = 0, J' = 20.5, -)$ and $A^2\Pi_{3/2}$ $(v'' = 0, J'' = 18.5, -)$ is forbidden, we use two optical transitions $R_{21}(20)$ ($X^2\Sigma^+_{1/2}$ $(v = 0, J = 19.5, +) \rightarrow A^2\Pi_{1/2}$ $(v' = 0, J' = 20.5, -)$: blue arrow) and $P_{22}(20)$ ($X^2\Sigma^+_{1/2}$ $(v = 0, J = 19.5, +) \rightarrow A^2\Pi_{3/2}$ $(v' = 0, J' = 18.5, -)$: orange arrow) near 359 nm to quantify the small energy gap between $A^2\Pi_{1/2}$ $(v' = 0, J' = 20.5, -)$ and $A^2\Pi_{3/2}$ $(v'' = 0, J'' = 18.5, -)$ (red arrow). The two optical transitions $R_{21}(20)$ and $P_{22}(20)$ originate from the same ground state $X^2\Sigma^+_{1/2}$ $(v = 0, J = 19.5, +)$, so the energy level interval of the two optical transitions just depends on the two different excited states.

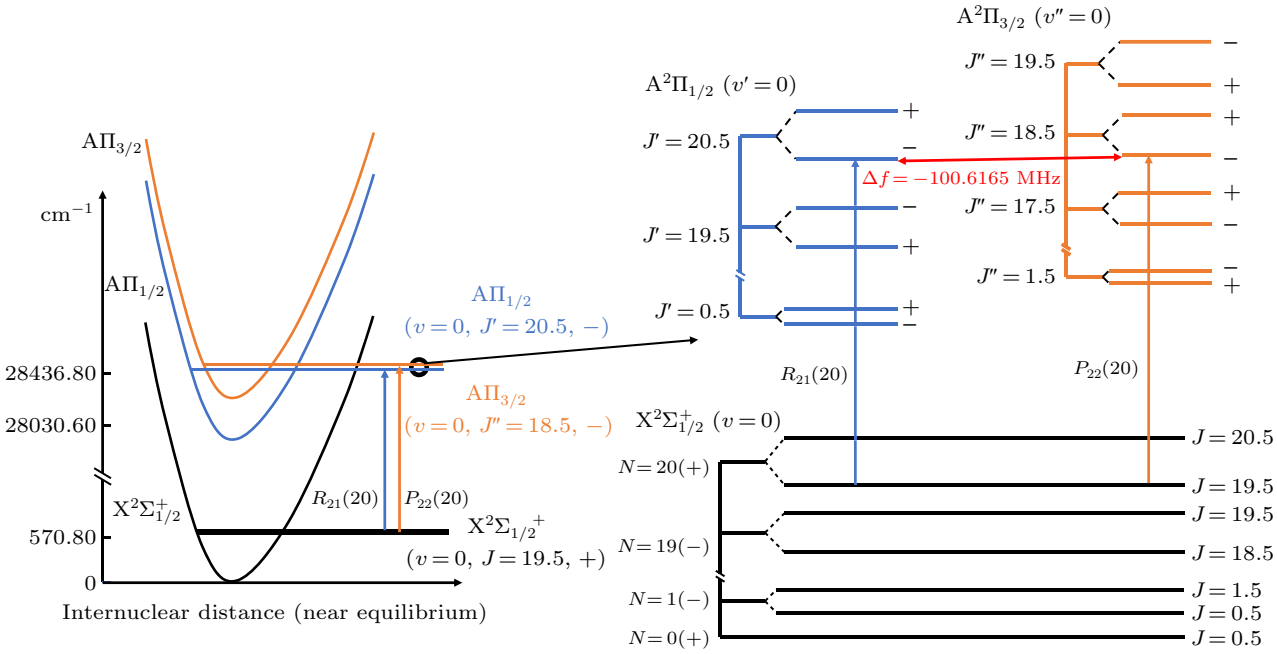


Fig. 2. Rotational energy levels of the $A^2\Pi$ and the $X^2\Sigma^+_{1/2}$ states and the selected optical transitions $R_{21}(20)$ ($X^2\Sigma^+_{1/2}$ $(v = 0, J = 19.5, +) \rightarrow A^2\Pi_{1/2}$ $(v' = 0, J' = 20.5, -)$: blue arrow) and $P_{22}(20)$ ($X^2\Sigma^+_{1/2}$ $(v = 0, J = 19.5, +) \rightarrow A^2\Pi_{3/2}$ $(v' = 0, J' = 18.5, -)$: orange arrow) with the small energy gap Δf between the constructed close-lying levels ($A^2\Pi_{1/2}$ $(v' = 0, J' = 20.5, -)$ and $A^2\Pi_{3/2}$ $(v'' = 0, J'' = 18.5, -)$: red arrow).

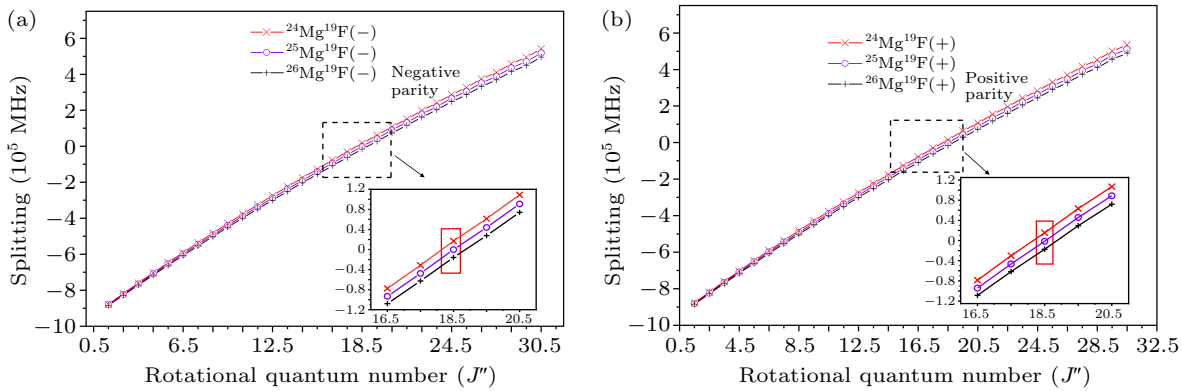


Fig. 3. Relationship of the rotational quantum number with the energy level interval between $A^2\Pi_{1/2}$ $J' = j + 2$ and $A^2\Pi_{3/2}$ $J'' = j$. $^{24}Mg^{19}F$, $^{25}Mg^{19}F$ and $^{26}Mg^{19}F$ are shown in red, purple and black lines, respectively. (a) Energy level interval between $A^2\Pi_{1/2}$ $J' = j + 2(-)$ and $A^2\Pi_{3/2}$ $J'' = j(-)$ between two negative parity states; the inset shows an enlargement. (b) Energy level interval between $A^2\Pi_{1/2}$ $J' = j + 2(+)$ and $A^2\Pi_{3/2}$ $J'' = j(+)$ between two positive parity states; the inset shows an enlargement. The points highlighted within a red square are the nearly degenerate situations.

Using the rotational Hamiltonian of $A^2\Pi$ in Eqs. (5) and (9), we can also get the nearly degenerate energy levels of different isotopes. The energy level intervals between $A^2\Pi_{1/2}$ $(v = 0, J' = j + 2)$ and $A^2\Pi_{3/2}$ $(v = 0, J'' = j)$ of different isotopes are shown in Fig. 3 as a function of rotational quantum number J''. The nearly degenerate situations occur when $J'' = 18.5$, highlighted within a red square. Using Eqs. (3) and (4), the minimum energy level interval Δf is expected when $A_v \approx 4B_v J''$, $\Delta f = A_v - 4B_v J''$, and the sensitivity is $K = A_v/\Delta f$. In Table 3, the different isotopes of

MgF are listed in the first column. The nearly degenerate levels of different isotopes and parities are listed in the second column. The third and fourth columns are the energy gaps and the corresponding sensitivity. We can know that the energy gap Δf between $A^2\Pi_{1/2}$ ($v'=0, J'=20.5, -$) and $A^2\Pi_{3/2}$ ($v''=0, J''=18.5, -$) in $^{25}Mg^{19}F$ is extremely small (~ -100 MHz), which can contribute to extremely high sensitivity ($|K| \sim 10^4$).

Table 3. Energy intervals of nearly degenerate levels in the $A^2\Pi$ state of different isotopes, together with their sensitivity K.

Isotope	Transition	f (MHz)	Sensitivity K
$^{24}Mg^{19}F$	$v'=0, J'=20.5, \Omega=1/2, + \rightarrow$ $v''=0, J''=18.5, \Omega=3/2, +$	16911.761	63
$^{24}Mg^{19}F$	$v'=0, J'=20.5, \Omega=1/2, - \rightarrow$ $v''=0, J''=18.5, \Omega=3/2, -$	15337.329	71
$^{25}Mg^{19}F$	$v'=0, J'=20.5, \Omega=1/2, + \rightarrow$ $v''=0, J''=18.5, \Omega=3/2, +$	−1571.4248	−694
$^{25}Mg^{19}F$	$v'=0, J'=20.5, \Omega=1/2, - \rightarrow$ $v''=0, J''=18.5, \Omega=3/2, -$	−100.61653	−10847
$^{26}Mg^{19}F$	$v'=0, J'=20.5, \Omega=1/2, + \rightarrow$ $v''=0, J''=18.5, \Omega=3/2, +$	−17250.639	−63
$^{26}Mg^{19}F$	$v'=0, J'=20.5, \Omega=1/2, - \rightarrow$ $v''=0, J''=18.5, \Omega=3/2, -$	−15872.353	−68

5. Estimation of the frequency uncertainties

This section discusses the frequency uncertainties in the transition from $X^2\Sigma^+_{1/2}$ ($v=0, J=19.5, +$) to $A^2\Pi_{3/2}$ ($v''=0, J''=18.5, -$) and the transition from $X^2\Sigma^+_{1/2}$ ($v=0, J=19.5, +$) to the $A^2\Pi_{1/2}$ ($v'=0, J'=20.5, -$) in $^{25}Mg^{19}F$. We mainly estimate the frequency uncertainties caused by the narrow linewidth, Zeeman shift, Stark shift, Doppler broadening and blackbody radiation.

The natural linewidth of MgF is in the MHz range. Our proposed method for spectral line measurement and natural linewidth is similar to that in Ref. [54], which the uncertainty in the spectral line measurement due to the natural linewidth is 1 kHz. Therefore, based on Ref. [54], we estimate that the uncertainty in the spectral line measurement due to the natural linewidth (δf_Γ) is about 1 kHz.

Usually, the Zeeman shift is caused by the different energy shifts in the upper and lower states:[45]

$$\delta f_Z = \frac{E_Z(\text{upper}) - E_Z(\text{lower})}{h}. \tag{10}$$

The $X^2\Sigma^+_{1/2}$ ($v=0, J=19.5, +$) state in Hund's coupling case (b),[51] the weak field Zeeman energy is given by

$$\Delta E_Z = \frac{g_S\left[J(J+1)+S(S+1)-N(N+1)\right]M_J\mu_B B_Z}{2J(J+1)}. \tag{11}$$

For $A^2\Pi$, the effective g-value for the rotational J is

$$g_J = \frac{g_L\Lambda + g_s\Sigma}{J(J+1)}\Omega. \tag{12}$$

The rotational Zeeman shift of $X^2\Sigma^+_{1/2}$ ($\Delta E_Z \propto 1/J$) and $A^2\Pi$ ($\Delta E_Z \propto 1/J'^2$) gradually decreases as J and J' increase. When the Earth's magnetic field is eliminated, choosing the states M_F close to zero, the Zeeman shift (δf_Z) can be narrower than 100 Hz when $J=19.5$.

The Stark shift for linear molecules is inversely proportional to $J(J+1)$. The Stark shift can be expressed as[55]

$$\delta f_S = \frac{(\mu E_0)^2}{B_v J(J+1)}, \tag{13}$$

where μ is electric dipole moment; E_0 is the amplitude of the optical field; h is Planck's constant; B_v is the rotational constant and J is the rotational quantum number. If we use a 10 mW probe laser, the total Stark shift (δf_S) is 2.45 Hz.

The transverse velocity of the molecular beam is very small and symmetrically distributed, so the average velocity in the transverse direction is zero; hence, there is no first-order Doppler effect. According to the second-order Doppler shift,

$$\Delta f_{2\text{ndDoppler}} = \frac{v^2}{2c^2}\omega_0. \tag{14}$$

If the transverse velocity of a collimated molecular beam is around ± 1 m/s, the second-order Doppler shift is 0.0046 Hz.

Blackbody radiation is always present in the experimental environment, so molecules will absorb blackbody photons, which will induce energy shifts on molecular energy levels. The blackbody radiation-induced energy shift for a quantum state $|i\rangle$ is given by

$$\Delta E_i = \frac{1}{6\pi^2\epsilon_0 c^3}\sum_j P\int_0^\infty \mathrm{d}\omega \frac{\omega^3\mu_{ij}^2}{\mathrm{e}^{\frac{\hbar\omega}{k_B T}}-1}\left(\frac{2\omega_{ij}}{\omega_{ij}^2-\omega^2}\right), \tag{15}$$

where $|\mu_{ij}|^2$ is the dipole moment matrix element between states i and j, ω_{ij} the transition frequency in circular frequency, T the ambient temperature and P the Cauchy principal value.[56] If we define $y = \frac{\hbar\omega_{ij}}{k_B T}$ and $x = \frac{\hbar\omega}{k_B T}$, according to the Farley–Wing function:

$$F(y) = \int_0^\infty \left(\frac{1}{y+x}+\frac{1}{y-x}\right)\frac{x^3\,\mathrm{d}x}{\mathrm{e}^x-1}. \tag{16}$$

We can transform Eq. (15) to

$$\Delta E_i = -\frac{1}{6\pi^2\epsilon_0 c^3}\left(\frac{k_B T}{\hbar}\right)^3\sum_j \mu_{ij}^2 F\left(\frac{\hbar\omega_{ij}}{k_B T}\right). \tag{17}$$

When the parameter $y \gg 1$, the Farley–Wing function can be approximated to

$$F(y) \approx \frac{2\pi^2}{15y}+\frac{16\pi^5}{63y^3}. \tag{18}$$

Thus, Eq. (17) can be expressed as

$$\Delta E_i = -\frac{1}{6\pi^2\epsilon_0 c^3}\left(\frac{k_B T}{\hbar}\right)^3$$

$$\times \sum_j \mu_{ij}^2 \left[\frac{2\pi^2}{15\frac{\hbar\omega_{ij}}{k_B T}} + \frac{16\pi^5}{63\left(\frac{\hbar\omega_{ij}}{k_B T}\right)^3} \right], \qquad (19)$$

where the room temperature T_c is about 300 K and the transition wavelength is about 359 nm ($y = \frac{\hbar\omega_{ij}}{k_B T} \gg 1$), the blackbody radiation shift (δf_b) is estimated to be 10^{-5} Hz.

In short, according to the reference,[12] the fractional temporal variation of μ is about 10^{-14} yr^{-1}. The sensitivity K in our scheme can reach up to 10^4, and the maximal allowable relative uncertainty is about $K \times (2\dot{\alpha}/\alpha + \dot{\mu}/\mu) \sim 10^{-10}$ yr^{-1}. The total frequency shifts ($\delta f = \delta f_\Gamma + \delta f_Z + \delta f_S + \delta f_{2\text{ndDoppler}} + \delta f_b$) are about 1 kHz from the above estimation of the frequency. Then, the relative uncertainty is about 1 kHz/($f(R_{21}(20))$) $=\sim 10^{-12}$ (or 1 kHz/$f(P_{22}(20))$ $=\sim 10^{-12}$) for the optical transition.

6. Conclusion

In conclusion, we propose a scheme to search for the variation of the fine-structure constant and the proton-to-electron mass ratio with time using MgF as a candidate. We find that the $A^2\Pi_{1/2}$ ($v' = 0, J' = 18.5, -$) state and the $A^2\Pi_{3/2}$ ($v'' = 0, J'' = 20.5, -$) state are nearly degenerate due to the contribution of the fine-structure and the rotational interval. According to the calculations, the energy gap between $A^2\Pi_{3/2}$ ($v' = 0, J' = 18.5, -$) and $A^2\Pi_{1/2}$ ($v'' = 0, J'' = 20.5, -$) in $^{25}Mg^{19}F$ is about 100 MHz, which contributes to a large sensitivity of 10^4. To quantify the small gap, we propose to use the two optical transitions, namely $X^2\Sigma^+_{1/2}$ ($v = 0, J = 19.5, +$) to $A^2\Pi_{3/2}$ ($v' = 0, J' = 18.5, -$) and $X^2\Sigma^+_{1/2}$ ($v = 0, J = 19.5, +$) to $A^2\Pi_{1/2}$ ($v'' = 0, J'' = 20.5, -$). We estimate the total frequency shifts caused by the Zeeman shift, AC Stark shift and blackbody radiation to be 600 Hz, which leads to a relative uncertainty of only 10^{-12}. Thus, the fractional temporal variation of μ is approximately better than 10^{-14} yr^{-1}. In summary, the $^{25}Mg^{19}F$ molecule appears to be a potential candidate for the detection of the variation of fundamental constants.

Acknowledgment

Project supported by the National Natural Science Foundation of China (Grant Nos. 12174115, 11834003, and 91836103).

References

[1] Cairncross W B and Ye J 2019 *Nat. Rev. Phys.* **1** 510
[2] Le D T 2024 *Sci. Rep.* **14** 15610
[3] Stadnik Y V and Flambaum V V 2015 *Phys. Rev. Lett.* **115** 201301
[4] Truppe S, Hendricks R J, Tokunaga S K, Lewandowski H J, Kozlov M G, Henkel C, Hinds E A and Tarbutt M R 2013 *Nat. Commun.* **4** 2600
[5] Hart L and Chluba J 2023 *MNRAS* **519** 3664
[6] Safronova M S, Budker D, DeMille D, Kimball D F J, Derevianko A and Clark C W 2018 *Rev. Mod. Phys.* **90** 025008
[7] Arvanitaki A, Huang J W and Tilburg K V 2015 *Phys. Rev. D* **91** 015015
[8] Hees A, Minazzoli O, Savalle E, Stadnik Y V and Wolf P 2018 *Phys. Rev. D* **98** 064051
[9] Zelevinsky T, Kotochigova S and Ye J 2008 *Phys. Rev. Lett.* **100** 043201
[10] DeMille D, Sainis S, Sage J, Bergeman T, Kotochigova S and Tiesinga E 2008 *Phys. Rev. Lett.* **100** 043202
[11] Shelkovnikov A, Butcher R J, Chardonnet C and Amy-Klein A 2008 *Phys. Rev. Lett.* **100** 150801
[12] Kobayashi J, Ogino A and Inouye S 2019 *Nat. Commun.* **10** 3771
[13] Kajita M 2009 *New J. Phys.* **11** 055010
[14] Rosenband T, Hume D B, Schmidt P O, Chou C W, Brusch A, Lorini L, Oskay W H, Drullinger R E, Fortier T M, Stalnaker J E, Diddams S A, Swann W C, Newbury N R, Itano W M, Wineland D J and Bergquist J C 2008 *Science* **319** 1808
[15] Schkolnik V, Budker D, Fartmann O, Flambaum V, Hollberg L, Kalaydzhyan T, Kolkowitz S, Krutzik M, Ludlow A and Newbury N 2023 *Quantum Sci. Technol.* **8** 014003
[16] Lange R, Huntemann N, Rahm J M, Sanner C, Shao H, Lipphardt B, Tamm C, Weyers S and Peik E 2021 *Phys. Rev. Lett.* **126** 011102
[17] Jansen P, Xu L H, Kleiner I, Ubachs W and Bethlem H L 2011 *Phys. Rev. Lett.* **106** 100801
[18] Ubachs W, Bagdonaite J, Salumbides E J, Murphy M T and Kaper L 2016 *Rev. Mod. Phys.* **88** 021003
[19] Leefer N, Weber C T M, Cingöz A, Torgerson J R and Budker D 2013 *Phys. Rev. Lett.* **111** 060801
[20] Figueroa N L, Berengut J C, Dzuba V, Flambaum V V, Budker D and Antypas D 2022 *Phys. Rev. Lett.* **128** 073001
[21] Hanneke D, Kuzhan B and Lunstad A 2021 *Quantum Sci. Technol.* **6** 014005
[22] Micheli A, Brennen G K and Zoller P 2006 *Nat. Phys.* **2** 341
[23] Bao Y C, Yu S S, Anderegg L, Chae E, Ketterle W, Ni K K and Doyle J M 2023 *Science* **382** 1138
[24] Ni K K, Rosenband T and Grimes D D 2018 *Chem. Sci.* **9** 6830
[25] Karman T, Tomza M and Pérez-Ríos J 2024 *Nat. Phys.* **20** 722
[26] Anderegg L, Vilas N B, Hallas C, Robichaud P, Jadbabaie A, Doyle J M and Hutzler N R 2023 *Science* **382** 665
[27] Cheuk L W, Anderegg L, Bao Y C, Burchesky S, Yu S S, Ketterle W, Ni K K and Doyle J M 2020 *Phys. Rev. Lett.* **125** 043401
[28] Ye J and Zoller P 2024 *Phys. Rev. Lett.* **132** 190001
[29] Flambaum V V and Kozlov M G 2007 *Phys. Rev. Lett.* **99** 150801
[30] Caldwell L, Roussy T S, Wright T, Cairncross W B, Shagam Y, Ng K B, Schlossberger N, Park S Y, Wang A Z, Ye J and Cornell E A 2023 *Phys. Rev. A* **108** 012804
[31] Beloy K, Kozlov M G, Borschevsky A, Hauser A W, Flambaum V V and Schwerdtfeger P 2011 *Phys. Rev. A* **83** 062514
[32] Beloy K, Borschevsky A, Schwerdtfeger P and Flambaum V V 2010 *Phys. Rev. A* **82** 022106
[33] Ganguly G, Sen A, Mukherjee M and Paul A 2014 *Phys. Rev. A* **90** 012509
[34] Nijs A J, Salumbides E J, Eikema K S E, Ubachs W and Bethlem H L 2011 *Phys. Rev. A* **84** 052509
[35] Hanneke D, Carollo R A and Lane D A 2016 *Phys. Rev. A* **94** 050101
[36] Pašteka L F, Borschevsky A, Flambaum V V and Schwerdtfeger P 2015 *Phys. Rev. A* **92** 012103
[37] Xu S P, Xia M, Yin Y N, Gu R X, Xia Y and Yin J P 2019 *J. Chem. Phys.* **150** 084302
[38] Xu S P, Xia M, Gu R X, Pei C Y, Yang Z H, Xia Y and Yin J P 2019 *J. Quant. Spectrosc. Ra.* **236** 106583
[39] Anderson M A, Allen M D and Ziurys L M 1994 *Astrophys. J.* **425** L53
[40] Xu S P, Xia M, Gu R X, Yin Y N, Xu L, Xia Y and Yin J P 2019 *Phys. Rev. A* **99** 033408
[41] Yan K, Gu R X, Wu D, Wei J, Xia Y and Yin J P 2022 *Front. Phys.* **17** 42502
[42] Ji Y B, Wei B, Guo H J, Liu Q, Yang T, Hou S Y and Yin J P 2022 *Chin. Phys. B* **31** 103201
[43] Bao Z B, Wang D F, Shao X P, Huang Y X and Yang X H 2023 *Chin. Phys. B* **32** 123302
[44] Ludlow A D, Boyd M M, Ye J, Peik E and Schmidt P O 2015 *Rev. Mod. Phys.* **87** 637
[45] Kajita M, Gopakumar G, Abe M, Hada M and Keller M 2014 *Phys. Rev. A* **89** 032509
[46] Brown J M and Carrington A 2003 *Rotational Spectroscopy of Diatomic Molecules* (1st edn.) (Cambridge University Press, Cambridge)
[47] Barrow R F and Beale J R 1967 *Proc. Phys. Soc.* **91** 483

[48] Watson J K G 1980 *J. Mol. Spectrosc.* **80** 411
[49] Dunham J L 1932 *Phys. Rev.* **41** 721
[50] Barnes M, Merer A J and Metha G F 1995 *J. Chem. Phys.* **103** 8360
[51] Brown J M, Kopp I, Malmberg C and Rydh B 1978 *Phys. Scr.* **17** 55
[52] Gu R X, Xia M, Yan K, Wu D, Wei J, Xu L, Xia Y and Yin J P 2022 *J. Quant. Spectrosc. Ra.* **278** 108015
[53] Chin C, Flambaum V V and Kozlov M G 2009 *New J. Phys.* **11** 055048
[54] Li R, Wu Y L, Rui Y, Li B, Jiang Y Y, Ma L S and Wu H B 2020 *Phys. Rev. Lett.* **124** 063002
[55] Townes C H and Schawlow A L 2012 *Microwave Spectroscopy* (2nd edn.) (New York: Dover Publications) p. 248249
[56] Norrgard E B, Eckel S P, Holloway C L and Shirley E L 2021 *New J. Phys.* **23** 033037
[57] Vanhaecke N and Dulieu O 2007 *Mol. Phys.* **105** 1723